

Spin-dependent γ softness or triaxiality in even-even $^{132-138}\text{Nd}$ nuclei*CHAI Qing-Zhen(柴清祯)¹ WANG Hua-Lei(王华磊)^{1,1)} YANG Qiong(杨琼)¹ LIU Min-Liang(柳敏良)²¹ School of Physics and Engineering, Zhengzhou University, Zhengzhou 450001, China² Institute of Modern Physics, Chinese Academy of Sciences, Lanzhou 730000, China

Abstract: The properties of γ instability in rapidly rotating even-even $^{132-138}\text{Nd}$ isotopes have been investigated using the pairing-deformation self-consistent total-Routhian-surface calculations in a deformation space of $(\beta_2, \gamma, \beta_4)$. It is found that even-even $^{134-138}\text{Nd}$ nuclei exhibit triaxiality in both ground and excited states, even up to high-spin states. The lightest isotope possesses a well-deformed prolate shape without a γ deformation component. The current numerical results are compared with previous calculations and available observables such as quadrupole deformation β_2 and the feature of γ -band levels, showing basically a general agreement with the observed trend of γ correlations (e.g. the pattern of the odd-even energy staggering of the γ band). The existing differences between theory and experiment are analyzed and discussed briefly.

Key words: even-even nucleus, total-Routhian-surface calculation, γ softness, triaxial deformation

PACS: 21.10.Re, 21.60.Cs, 21.60.Ev **DOI:** 10.1088/1674-1137/39/2/024101

1 Introduction

Atomic nuclei exhibit a variety of shapes which are generally sensitive to the single-particle structure, the collective behavior and the total angular momentum. Studies have revealed that most deformed nuclei have axially symmetric shapes (prolate or oblate), which is confirmed by the observation of rotational band structures and measurements of their properties [1]. Nevertheless, evidence for nonaxial γ deformations (or softness) has so far been widely found in nuclear spectroscopy. For instance, some unexpected characteristics possibly caused by γ deformations, such as wobbling, signature inversion (or splitting) and chiral doublets, have been observed in many nuclei [2–4]. One would expect that potential energy surfaces that are γ soft or which display deep minima with nonzero γ value would produce rather different nuclear spectra, but this is not the case [5]. Indeed, the question of whether non-axially-symmetric nuclei are γ soft or triaxial has been an ongoing and active issue in nuclear structure physics for over 50 years. It has been investigated extensively using theoretical approaches that are essentially based on a rigid triaxial potential [6] and a completely γ -flat (γ -unstable) potential [7]. A further discussion on signatures of γ softness or triaxiality in low energy nuclear spectra was performed about 20 years ago by Zamfir and Casten [5]. During the past several decades, numerous studies have been carried

out in terms of various theoretical approaches including mean-field models and beyond mean-field models (see [8–11] and references therein). More recently, the triaxial projected shell model (TPSM) [12] and total-Routhian-surface (TRS) [13] calculations have been carried out for even-even germanium and selenium isotopes to investigate the nature of γ deformation and search for possible stable triaxial deformations of nuclear states. The TPSM calculations for ^{138}Nd have also been performed where the yrast and 1γ bands are reproduced excellently [14].

However, despite considerable effort, the precise description of axially asymmetric shapes and the resulting triaxial quantum many-body rotors still remains an open problem. It is well known that many of the nuclei in the $A=130-140$ mass transitional region show the interesting characteristic feature known as triaxiality, or a high degree of γ -softness, which arises from the interplay of the valence protons and neutrons occupying respectively low-lying and high-lying Nilsson orbitals within the $h_{11/2}$ j -shell [15]. Their nuclear spectra can usually be satisfactorily described using the corresponding $O(6)$ dynamical symmetry of the interacting boson model [16]. In the present work, we perform TRS calculations with the inclusion of the γ deformation for several selected even-even $^{132-138}\text{Nd}$ isotopes in this mass region, focusing on their evolution of γ -softness or triaxiality with rotation and providing a test for the present model. We have previously investigated the evolution of octupole-softness in

Received 25 April 2014

* Supported by National Natural Science Foundation of China (10805040,11175217), Foundation and Advanced Technology Research Program of Henan Province(132300410125) and S & T Research Key Program of Henan Province Education Department (13A140667)

1) E-mail: wanghualai@zzu.edu.cn

©2015 Chinese Physical Society and the Institute of High Energy Physics of the Chinese Academy of Sciences and the Institute of Modern Physics of the Chinese Academy of Sciences and IOP Publishing Ltd

rotating $^{106,108}\text{Te}$ and neutron-deficient U isotopes using similar TRS calculations [17, 18]. Experimentally, the high-spin behaviors in even-even nuclei have been studied and interpreted on the basis of triaxial shapes in [19–23]. Moreover, the quasi- γ bands have been identified in these nuclei [16, 23–26], and even the multiphonon γ -vibrational band in ^{138}Nd [14].

2 The theoretical framework

The TRS calculation applied here is based on the pairing-deformation-frequency self-consistent cranked shell model [27, 28]. Such an approach usually accounts well for the overall systematics of high-spin phenomena in rapidly rotating medium and heavy mass nuclei. The total Routhian, which is called ‘Routhian’ rather than ‘energy’ in a rotating frame of reference, is the sum of the energy of the non-rotating state and the contribution due to cranking,

$$E^\omega(Z, N, \hat{\beta}) = E^{\omega=0}(Z, N, \hat{\beta}) + [\langle \Psi^\omega | \hat{H}^\omega(Z, N, \hat{\beta}) | \Psi^\omega \rangle - \langle \Psi^\omega | \hat{H}^\omega(Z, N, \hat{\beta}) | \Psi^\omega \rangle^{\omega=0}]. \quad (1)$$

The energy $E^{\omega=0}(Z, N, \hat{\beta})$ of the non-rotating state consists of a macroscopic part, being a smooth function of Z , N and deformation, and a fluctuating microscopic part, which is based on some phenomenological single-particle potential, that is,

$$E^{\omega=0}(Z, N, \hat{\beta}) = E_{\text{macr}}(Z, N, \hat{\beta}) + E_{\text{micr}}(Z, N, \hat{\beta}). \quad (2)$$

where the macroscopic term is obtained from the sharp-surface standard liquid-drop formula with the parameters used by Myers and Swiatecki [29]. The microscopic correction part, which arises because of the non-uniform distribution of single-particle levels in the nucleus, mainly contains a shell correction and a pairing correction:

$$E_{\text{micr}}(Z, N, \hat{\beta}) = \delta E_{\text{shell}}(Z, N, \hat{\beta}) + \delta E_{\text{pair}}(Z, N, \hat{\beta}). \quad (3)$$

These two contributions can both be evaluated from a set of single-particle levels. Cranking indicates that the nuclear system is constrained to rotate around a fixed axis (e.g. the x -axis) at a given frequency ω . This is equivalent to minimizing the rotation Hamiltonian $H^\omega = H - \omega I_x$ instead of the Hamiltonian H with respect to variations of the mean field. For a given rotational frequency and point of deformation lattice, this can be achieved by solving the well known Hartree-Fock-Bogolyubov–Cranking (HFBC) equations using a sufficiently large space of single-particle states. Then one can obtain the energy relative to the non-rotating state at $\omega=0$, as mentioned in Eq. (1). After the numerical calculated Routhians at fixed ω are interpolated using a cubic spline function between the lattice points, the equilibrium deformation can be determined by minimizing the calculated TRS.

Note that nuclear shape is defined by the standard parametrization in which it is expanded in spherical harmonics $Y_{\lambda\mu}(\theta, \phi)$ [30]. There is a fundamental limitation in λ , because the range of the individual ‘bumps’ on the nuclear surface decreases by increasing λ and obviously should not be smaller than a nucleon diameter [31]. A limiting value of $\lambda < A^{1/3}$ can be obtained by a crude estimate [31]. Therefore, the deformation parameter $\hat{\beta}$ includes β_2 , γ , and β_4 where γ describes triaxial shapes. The single-particle energies needed above are obtained from a phenomenological Woods-Saxon (WS) potential [30, 32] with the parameter set widely used for cranking calculations. During the diagonalization process of the WS Hamiltonian, deformed harmonic oscillator states with the principal quantum number $N \leq 12$ and 14 have been used as a basis for protons and neutrons, respectively. The shell and pairing corrections at each deformation point are calculated using the Strutinsky method [33] and Lipkin-Nogami (LN) method [34], respectively. The Strutinsky smoothing is performed with a sixth-order Laguerre polynomial and a smoothing range $\gamma = 1.20\hbar\omega_0$, where $\hbar\omega_0 = 41/A^{1/3}$ MeV. The LN method avoids the spurious pairing phase transition encountered in the simpler Bardeen-Cooper-Schrieffer calculation. In the pairing windows, dozens of single-particle levels, the respective states (e.g. half of the particle number Z or N) just below and above the Fermi energy, are included empirically for both protons and neutrons. Moreover, not only monopole but also doubly stretched quadrupole pairings are considered. The monopole pairing strength, G , is determined by the average gap method [35] and the quadrupole pairing strengths are obtained by restoring the Galilean invariance broken by the seniority pairing force [36]. Certainly, pairing correlations are dependent on rotational frequency as well as deformation. While solving the HFBC equations, pairing is treated self-consistently and symmetries of the rotating potential are used to simplify the cranking equations. In the reflection-symmetric case, both signature, r , and intrinsic parity, π are good quantum numbers.

3 Results and discussions

The present TRS method, similar to most of the existing cranking calculations, assumes that the rotational axis coincides with one of the principal axes (the x axis is generally chosen) of the triaxial potential including β_2 , γ , and β_4 deformations. In the actual calculations the Cartesian quadrupole coordinates $X = \beta_2 \cos(\gamma + 30^\circ)$ and $Y = \beta_2 \sin(\gamma + 30^\circ)$ were used, where the parameter β_2 specifies the magnitude of the quadrupole deformation, while γ specifies the asymmetry of the shape. In the Lund convention adopted here, the triaxiality pa-

parameter covers the range $-120^\circ \leq \gamma \leq 60^\circ$ and the three sectors $[-120^\circ, -60^\circ]$, $[-60^\circ, 0^\circ]$ and $[0^\circ, 60^\circ]$ represent the same triaxial shapes but represent rotation about the long, medium and short axes, respectively. Certainly, for $\gamma = -120^\circ$ (prolate shape) the nucleus rotates around the prolate symmetry axis and for $\gamma = 60^\circ$ (oblate shape) it rotates around the oblate symmetry axis. For $\gamma = 0^\circ$ (prolate shape) and for $\gamma = -60^\circ$ (oblate shape) the nucleus has a collective rotation around an axis perpendicular to the symmetry axis.

Figure 1 shows the equilibrium deformation parameters β_2 and γ obtained from the calculated TRS minima for frequencies ranging from $\hbar\omega = 0.0$ to 0.5 MeV (the corresponding spin maximum of even-even $^{132-138}\text{Nd}$ can be extended up to about $20, 22, 16$ and $14\hbar$, respectively). Their ground-state values are compared with other calculations and experiments [37–39], showing that our results are close to the experimental values though there is still a systematic underestimation for β_2 . The negative β_2 of ^{138}Nd given by Möller et al. [37] indicates this nucleus is oblate, which differs from our results and experiments. As expected, the ground-state β_2 deformations of these nuclei increase as the neutron number N moves away from the closed shell $N=82$. The calculated γ values are generally in agreement with the calculations by Möller et al. [38], except for the result for ^{134}Nd . Note that a nucleus with $\pm\gamma$ deformations (e.g. ^{138}Nd) has the same shape, as mentioned above. The β_2 deformations in these nuclei stay almost constant as a function of

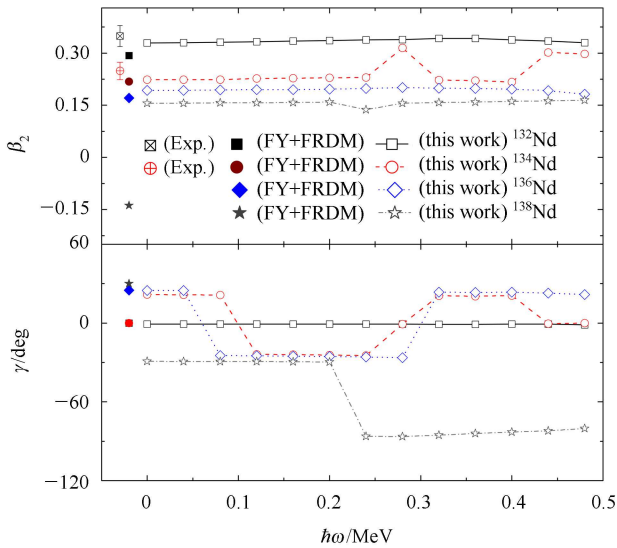


Fig. 1. Calculated deformation parameters β_2 (top) and γ (bottom) of yrast states for even-even nuclei $^{132-138}\text{Nd}$ as a function of the rotational frequency $\hbar\omega$, compared with the FY +FRDM calculations [37, 38] and partial experimental values obtained from reduced transition probabilities $B(E2)$ for the ground states [39].

rotational frequency. The change of γ value may provide the evolution information for the triaxial shape and rotational axis. As shown in Fig. 1, it can be easily found that ^{132}Nd has a prolate shape with $\gamma = 0^\circ$. $^{134,136}\text{Nd}$ exhibit the evolutions of the rotational axes from the short-axis to the medium-axis to the short-axis; moreover, ^{134}Nd has a prolate collective rotation beyond $\hbar\omega = 0.4$ MeV. For ^{138}Nd , the nucleus, with $\gamma \approx -29^\circ$, first rotates around the medium axis, then a shape transition from prolate-triaxial to oblate-triaxial takes place at $\hbar\omega \approx 0.2$ MeV; the nucleus, now with $\gamma \approx -84^\circ$, then begins to rotate around the long axis.

For transitional nuclei, the level scheme is more complicated than that of spherical or well-deformed nuclear shapes. Theoretical studies are usually model-dependent because their equilibrium shapes are generally soft and strongly affected by the mean-field and pairing potential parameters. However, the rigidity or softness of the nucleus, which cannot be seen in Fig. 1, is almost independent of model parameters. To visually display the nuclear softness in both β_2 and γ directions, we show the corresponding deformation energy curves (the total Routhian curve along the minimum valley of the TRS) in Figs. 2 and 3. At each nucleus, four typical rotational frequencies are selected to investigate the softness evolution with rotation. One can see that the rotational effects on the quadrupole deformation β_2 are small, as shown in Fig. 2, implying that the shapes are basically rigid against β_2 variation. Fig. 3 shows that the energy curves as a function of γ deformation, on the other hand, are strongly affected by the cranking. At the ground states, the triaxial minima are rather shallow. Theoretical and

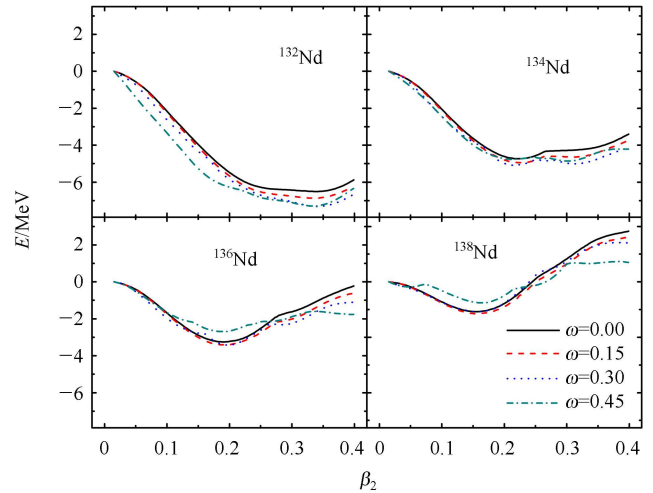


Fig. 2. Total deformation Routhian curves against β_2 for even-even $^{132-138}\text{Nd}$ nuclei at several selected rotational frequencies $\omega = 0.00$ (solid lines), 0.15 (dash lines), 0.30 (dot lines) and 0.45 (dash-dot lines) MeV/\hbar . At each β_2 point, the energy has been minimized with respect to γ and β_4 .

systematic studies indicate that the $N = 76$ nuclei are more γ -rigid than their neighbors with other neutron numbers [25, 40]. It seems that the depth of the triaxial minimum in $^{136}\text{Nd}_{76}$ is indeed the largest. The evolution of the softness and depth of the minimum is clearly presented under rotation, including that of the non-yrast minimum. For instance, the prolate-oblate shape coexistence observed in experiments [41] can be found in ^{134}Nd , as shown in Fig. 3, and a similar situation exists in ^{132}Nd . In $^{136,138}\text{Nd}$, the coexistence of prolate-triaxial and oblate-triaxial shapes is possible and awaits experimental confirmation.

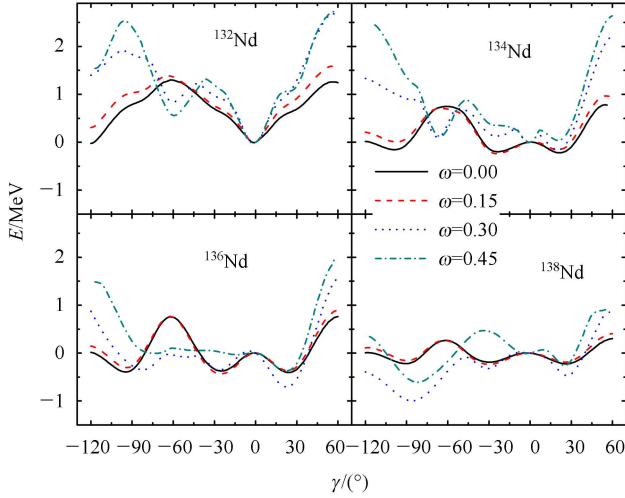


Fig. 3. Similar to Fig. 2, but with total deformation Routhian curves against γ deformation.

The quantity $E_s/E(2_1^+)$, $E_s = E(2_2^+) - E(4_1^+)$, can be as a global signature of the structural evolution involving axial asymmetry [43]. In the extreme γ -unstable limit [7], the value of $E_s/E(2_1^+)$ is zero due to the completely degenerate 2_2^+ and 4_1^+ states. In the case of rigid-triaxial rotor with $25^\circ \leq \gamma \leq 30^\circ$ [6], the 2_2^+ state goes under the 4_1^+ level and reaches the bottom at the extreme of triaxiality with $\gamma = 30^\circ$ ($E_s/E(2_1^+) = -0.67$). Therefore, nuclei with negative values of $E_s/E(2_1^+)$ between these two extremes 0 and -0.67 are most likely to be characterized by γ -soft potentials with shallow minima at the average γ value close to 30° . Meanwhile, the positive value of $E_s/E(2_1^+)$ indicates that the nucleus possesses an axially-symmetric shape, because the 2_2^+ state lies at high excitation energy relative to the 2_1^+ and 4_1^+ states.

The empirical $E_s/E(2_1^+)$ values for even-even $^{132-138}\text{Nd}$ are presented in Fig. 4, which also shows the results for their adjacent nuclei $^{128-134}\text{Ba}$, $^{130-136}\text{Ce}$, $^{136,138}\text{Sm}$ and $^{140,142}\text{Gd}$. One can see a general decrease in $E_s/E(2_1^+)$ with increasing N , which illuminates the increasing of γ softness in these isotopes. The observed rapid decrease from 0.99 (^{132}Nd) to -0.45 (^{138}Nd) in

$E_s/E(2_1^+)$ in the Nd isotopic chain reflects the structural change from a nearly axial rotor with the small-amplitude γ vibrations to a large-amplitude γ -soft dynamics. The γ -soft properties of even-even $^{134-138}\text{Nd}$, as shown in Fig. 3, are also supported by the negative $E_s/E(2_1^+)$ values. The $E_s/E(2_1^+)$ value in ^{138}Nd is somewhat smaller than the empirical value of $E_s/E(2_1^+) \approx 0.5$, which is characteristic of the critical-point nuclei in terms of maximum γ softness between prolate and oblate shapes. It should be noted that a critical point of a prolate to oblate phase transition in γ -soft nuclei is discussed in the context of the $O(6)$ limit of the interacting boson model, along with an interpretation in terms of Landau theory. This is in good agreement with our calculated results of $\gamma \sim 29^\circ$ in the ground state, as shown in Fig. 1. Our calculations show that the quantum phase transition from triaxial-prolate to triaxial-oblate shapes in ^{138}Nd occurs at low-lying rather than ground states. The calculations of Möller et al. [37] indicate, however, that such a phase transition has already taken place in ^{138}Nd ($\beta_2 < 0$). Fig. 4 also shows that ^{138}Nd with the lowest $E_s/E(2_1^+)$ value is the γ -softest nucleus in this mass region. Indeed, ^{138}Nd exhibits rather γ -vibrational behavior experimentally, as demonstrated by the observation of the properties expected for rotational bands built on one- γ and two- γ -phonon states [14]. This is also supported by the study of Gizon et al. [44] where it is deduced that a shape change across $\gamma \approx 30^\circ$ from prolate to oblate occurs between the $N=77$ and $N=79$ Nd isotopes.

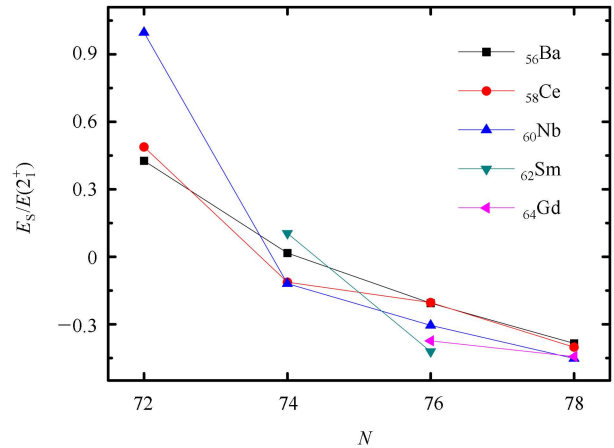


Fig. 4. Empirical values of the quantity $E_s/E(2_1^+)$ for even-even Nd and its adjacent Ba, Ce, Sm and Gd isotopes versus neutron number. The available experimental data are taken from [14, 16, 23–26, 42].

The energy staggering of the odd- and even-spin levels of a γ band can usually be viewed as an important structural indicator to distinguish between γ -rigid and γ -soft asymmetry [5]. In two such different cases, though

the energies of the ground-state band are similar, the γ band nevertheless exhibits a different energy staggering. That is, the γ -band levels of a rigid triaxial potential form couplets arranged as $(2_\gamma^+, 3_\gamma^+)$, $(4_\gamma^+, 5_\gamma^+)$, $(6_\gamma^+, 7_\gamma^+)$, ... while for a completely γ -flat potential it has couplets (2_γ^+) , $(3_\gamma^+, 4_\gamma^+)$, $(5_\gamma^+, 6_\gamma^+)$, ... Therefore, odd-even staggering in a γ band can be studied using the quantity [45]

$$S(I) = \frac{E(I_\gamma^+) + E[(I-2)_\gamma^+] - 2E[(I-1)_\gamma^+]}{E(2_1^+)}, \quad (4)$$

in which the energy differences are normalized to $E(2_1^+)$. Obviously, the sign of $S(I)$ is a strong indicator of the nature of the γ degree of freedom. For a rigid triaxial potential, $S(I)$ will exhibit an oscillating behavior that takes on positive and negative values for even and odd spins, respectively. In both the vibrator and limits, an opposite phase appears in $S(I)$, namely positive for odd spin and negative for even spin. Moreover, the overall magnitude of $S(I)$ is larger in the γ -soft limit and increases gradually with spin compared with the vibrator predictions that are smaller in magnitude and constant. For an axially symmetric deformed rotor, the $S(I)$ values are positive, small, and constant as a function of spin [45].

Experimental staggering $S(I)$ for even-even $^{132-138}\text{Nd}$ nuclei are shown in Fig. 5 in comparison with those for a rigid triaxial nucleus ^{76}Ge [46] and an axially symmetric nucleus ^{162}Er [45]. It is unambiguous that the sign of $S(4)$ is negative for the Nd isotopes. The magnitude of

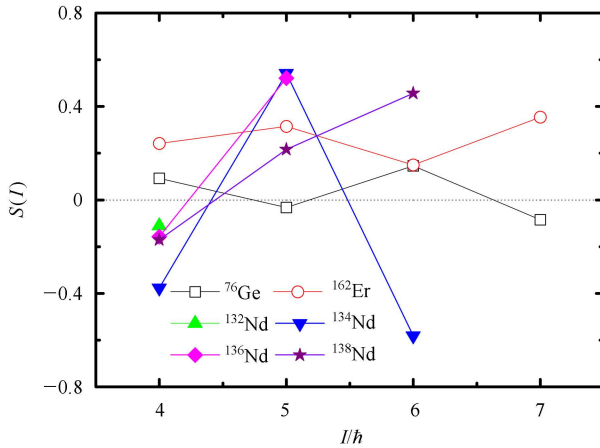


Fig. 5. Odd-even energy staggering $S(I)$ for even-even $^{132-138}\text{Nd}$ nuclei, together with the γ -rigid nucleus ^{76}Ge and axially-symmetric nucleus ^{162}Er for comparison. These available data are from [14, 23–26, 45, 46]

$S(4)$ is smallest for ^{132}Nd and largest for ^{134}Nd . The oscillatory pattern of $S(I)$ observed in ^{134}Nd and at least $S(4)$ and $S(5)$ in $^{136,138}\text{Nd}$, opposite to that in ^{76}Ge , agrees with the γ -soft potential predictions. The overall magnitude of the staggering displays an increasing trend with spin I except for ^{132}Nd in which only one $S(4)$ point is plotted due to the scarce data. Especially for ^{136}Nd , one can see a rapidly increasing staggering which may indicate the γ softness increases with the increasing spin. It should be noted that if the experimental data suggested in [14] are used the $S(6)$ value will be positive, which is not expected for a γ -soft case. If this is actually the case, it will be necessary to reveal the mechanism behind this anomalous behavior. These properties are basically consistent with the ω -dependent energy curves, as shown in Fig. 3. To investigate the evolution of γ softness with rotation, it will be of interest to further identify the high-spin levels of the γ band in future experiments.

4 Summary

In summary, doubly even $^{132-138}\text{Nd}$ nuclei have been investigated in terms of the TRS calculations in the $(\beta_2, \gamma, \beta_4)$ deformation space, focusing on the evolution of the γ -softness and triaxiality with rotation. Compared to other calculations and experiments, the equilibrium deformation parameter β_2 and γ are evaluated and it indicates that our results are closer to the experimental values. In these soft nuclei, the existing differences in the equilibrium β_2 and γ deformations between the present work and other calculations may be, to a large extent, attributed to model parameters. The nuclear softness in the β_2 and γ directions are displayed using the corresponding energy curves at several selected rotational frequencies. As important structural indicators of axial asymmetry, the quantities $S(I)$ and $E_s/E(2_1^+)$ are analyzed and discussed. The general trends are in agreement with our calculations. Meanwhile, it is pointed out that more detailed data, especially in the γ band, is needed to investigate and confirm the γ -softness evolution in $^{132-138}\text{Nd}$. Also, it should be noted that the present method does not include the effects of rotation-vibration coupling, nor does it include a tilted-axis-tilting calculation, but it can provide a qualitative description of γ correlations that are at least consistent to some extent with several observed properties. A more complete calculation, which we hope to do in future work, should take these effects into account, especially for the transitional soft nuclei.

References

- 1 Stránský P, Frank A, Bijker R. *J. Phys.: Conf. Ser.*, 2011, **322**: 012018
- 2 Ödegård S W, Hagemann G B, Jensen D R et al. *Phys. Rev. Lett.*, 2001, **86**: 5866–5869
- 3 Bengtsson R, Frisk H, May F R et al. *Nucl. Phys. A*, 1984, **415**: 189–214
- 4 Starosta K, Koike T, Chiara C J et al. *Phys. Rev. Lett.*, 2001, **86**: 971–974
- 5 Zamfir N V, Casten R F. *Phys. Lett. B*, 1991, **260**: 265–270
- 6 Davydov A S, Filippov G F. *Nucl. Phys.*, 1958, **8**: 237–249
- 7 Wilets L, Jean M. *Phys. Rev.*, 1956, **102**: 788–796
- 8 Bender M, Heenen P H, Reinhard P G. *Rev. Mod. Phys.*, 2003, **75**: 121–180
- 9 Frauendorf S. *Rev. Mod. Phys.*, 2001, **73**: 463–514
- 10 LI Z P, Nikšić T, Vretenar D et al. *Phys. Rev. C*, 2010, **81**: 064321
- 11 YAO J M, MENG J, RING P et al. *Phys. Rev. C*, 2009, **79**: 044312
- 12 Bhat G H, Dar W A, Sheikh J A et al. *Phys. Rev. C*, 2014, **89**: 014328
- 13 SHEN S F, ZHENG S J, XU F R et al. *Phys. Rev. C*, 2011, **84**: 044315
- 14 LI H J, XIAO Z G, ZHU S J et al. *Phys. Rev. C*, 2013, **87**: 057303
- 15 CHEN Y S, Frauendorf S, Leander G A. *Phys. Rev. C*, 1983, **28**: 2437–2445
- 16 Saito T R, Saito N, Starosta K et al. *Phys. Lett. B*, 2008, **669**: 19–23
- 17 WANG H L, LIU H L, XU F R et al. *Prog. Theo. Phys.*, 2012, **128**: 363–371
- 18 WANG H L, LIU H L, XU F R. *Phys. Scr.*, 2012, **86**: 035201
- 19 Petrache C M, Bazzacco D, Lunardi S et al. *Phys. Lett. B*, 1996, **387**: 31–36
- 20 Mukhopadhyay S, Almeded D, Garg U et al. *Phys. Rev. C*, 2008, **78**: 034311
- 21 Petrache C M, Bianco G L, Ward D et al. *Phys. Rev. C*, 1999, **61**: 011305(R)
- 22 Wadsworth R, O'Donnell J M, Watson D L et al. *Nucl. Phys.*, 1988, **14**: 239–251
- 23 Angelis G D, Cardona M A, Poli M D et al. *Phys. Rev. C*, 1994, **49**: 2990–2999
- 24 Paul E S, Beausang C W, Fossan D B et al. *Phys. Rev. C*, 1987, **36**: 1853–1859
- 25 Kortelahti M O, Kern B D, Braga R A et al. *Phys. Rev. C*, 1990, **42**: 1267–1278
- 26 Petrache C M, Frauendorf S, Matsuzaki M et al. *Phys. Rev. C*, 2012, **86**: 044321
- 27 Satuła W, Wyss R, Magierski P. *Nucl. Phys. A*, 1994, **578**: 45–61
- 28 XU F R, Satuła W, Wyss R. *Nucl. Phys. A*, 2000, **669**: 119–134
- 29 Myers W D, Swiatecki W J. *Nucl. Phys.*, 1966, **81**: 1–60
- 30 Ćwiok S, Dudek J, Nazarewicz W et al. *Comp. Phys. Comm.*, 1987, **46**: 379–399
- 31 Greiner W, Maruhn J A. *Nuclear Models*, Berlin: Springer, 1996. 108–115
- 32 Nazarewicz W, Wyss R, Johnson A. *Nucl. Phys. A*, 1989, **503**: 285–330
- 33 Strutinsky V M. *Nucl. Phys. A*, 1967, **95**: 420–442
- 34 Pradhan H C, Nogami Y, Law J. *Nucl. Phys. A*, 1973, **201**: 357–368
- 35 Möller P, Nix J R. *Nucl. Phys. A*, 1992, **536**: 20–60
- 36 Sakamoto H, Kishimoto T. *Phys. Lett. B*, 1990, **245**: 321–324
- 37 Möller P, Nix J R, Myers W D et al. *At. Data Nucl. Data Tables*, 1995, **59**: 185–381
- 38 Möller P, Bengtsson R, Carlsson B G et al. *At. Data Nucl. Data Tables*, 2008, **94**: 758–782
- 39 Raman S, Nestor Jr. C W, Tikkanen P. *At. Data Nucl. Data Tables*, 2001, **78**: 1–128
- 40 Kern B D, Mlekodaj R L, Leander G A et al. *Phys. Rev. C*, 1987, **36**: 1514–1521
- 41 Petrache C M, SUN Y, Bazzacco D et al. *Nucl. Phys. A*, 1997, **617**: 249–264
- 42 [//www.nndc.bnl.gov/](http://www.nndc.bnl.gov/)
- 43 Watanabe H, Yamaguchi K, Odahara et al. *Phys. Lett. B*, 2011, **704**: 270–275
- 44 Gizon J, Gizon A, Diamond R M et al. *Nucl. Phys.*, 1978, **4**: L171–L175
- 45 McCutchan E A, Bonatsos D, Zamfir N V et al. *Phys. Rev. C*, 2007, **76**: 024306
- 46 Toh Y, Chiara C J, McCutchan E A et al. *Phys. Rev. C*, 2013, **87**: 041304(R)